Terahertz-wave generation by surface-emitted four-wave mixing in optical fiber

Ping Zhou (周 萍)* and Dianyuan Fan (范滇元)

Shanghai Institute of Optics and Fine Mechanics, Chinese Academy of Sciences, Shanghai 201800, China

**Corresponding author: zhoup0615@163.com*

Received November 16, 2010; accepted December 17, 2010; posted online April 18, 2011

We propose a novel terahertz-wave source through the four-wave mixing effect in a conventional single-mode optical fiber pumped by a dual-wavelength laser whose difference frequency lies in the terahertz range. Surface-emitted geometry is employed to decrease absorption loss. A detailed derivation of the terahertz-wave power expression is presented using the coupled-wave theory. This is a promising way for realizing a reasonable narrow-band terahertz-wave source.

OCIS codes: 190.0190, 060.0060.

doi: 10.3788/COL201109.051902.

Narrow-band or continuous wave (CW) terahertz (THz) signals are of considerable importance for high-resolution THz spectroscopy, THz sensors and ultrabroadband communications[1−4]. Nonlinear optical methods are effective and important techniques for narrow-band THz-wave generation[5−7]. However, the THz-wave generation by the difference-frequency generation (DFG) or optical parametric oscillation (OPO) is difficult to increase the conversion efficiency. There are two major obstacles. Firstly, due to the fact that the refractive index varies significantly in the infrared and THz regions in nonlinear optical crystals, the previous experiments have been made only in the totally non-collinear configuration, which limits the interplay of the THz wave with the optical waves. The second is the high attenuation in the THz region. For example, the widespread $LiNbO_3$ crystals have an absorption coefficient of about 30 cm^{-1}[8]. This limits the crystal length and hence the conversion efficiency. Although the quasi-phase matching scheme has been applied to realize the collinear DFG or OPO[9], it still suffers from the high attenuation in crystals. In other work, the surface-emitted geometry has been demonstrated in periodically poled $LiNbO_3$ (PPLN) to overcome the high absorption loss[10]. Unfortunately, this method requires complex crystal fabrication and the interaction length is limited by the size of the base material.

In this letter, we present a new narrow-band THz-wave source based on a conventional optical fiber. Three infrared optical waves are coupled into an optical fiber to generate a narrow-band THz-wave signal through the four-wave mixing (FWM) process. The surface-emitted configuration has been applied to minimize the absorption loss of the THz wave in materials. Unlike those methods aforementioned, our approach makes the pump and signal optical wave parallel which increases greatly the interaction length of the nonlinear process. Moreover, the optical fibers are widely used in telecommunications equipment and have the potential to use commercial technologies, such as highly stable diode lasers and high power optical amplifiers. This approach is a promising way to realize a miniaturized, narrow-band THz source with relatively high output power.

The principle of the novel THz generator is demonstrated in Fig. 1. A dual-wavelength laser whose difference frequency lies in the THz range has been used to produce the 10-ns near infrared (NIR) pulses. One of the two wavelengths is set to be frequency tunable. The two optical waves are amplified by the Er-doped fiber amplifiers (EDFAs), and then a second harmonic wave of the lower frequency light is generated through a β-barium borate (BBO) crystal. Then the three optical waves are merged into a polarization maintaining (PM) optical fiber and the THz radiation is generated by the four-wave mixing effect. The envelope of the THz signal is a pulse with duration of ∼10 ns, so that the THz signal oscillating at a ps scale can be viewed as a CW signal.

Due to the absorption coefficient of the optical fibers in THz range is still considerably large (5 cm^{-1}), the THz radiation generated in the collinear geometry can be subsequently absorbed. Hence the surface-emitted geometry is applied to decrease absorption loss. The surface-emitted generation means that the THz wave radiates from the surface of the optical fiber and propagates perpendicular to the direction of the pump optical waves. The surface-emitted geometry has been widely demonstrated in several types of crystals to generate THz wave by the second-order nonlinear process in recent years[11,12]. If the third-order polarization caused by the three NIR waves in the optical fiber has the same phase at any point in the longitudinal propagation direction, the radiated THz-wave can interfere constructively only in the lateral direction. The phase mismatch in the lateral direction can be compensated through periodical polarization in slanted PPLN and 2-D PPLN, or through the momentum uncertainty caused by the strongly

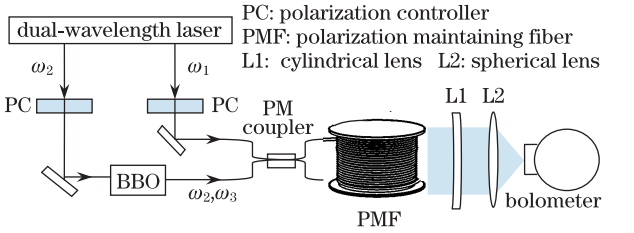

Fig. 1. Schematic of the surface-emitted FWM in optical fibers.

focused beams[13]. In our case, the single-mode optical fiber has several μm-mode field diameters, which is much less than the effective wavelength of THz wave in fibers, so the momentum uncertainty is enough to compensate the phase mismatch in the lateral direction. The THz radiation from the surface of the optical fiber coil is focused by a cylindrical lens and a spherical lens, and then detected with a Si bolometer, cooled at 4.2 K.

Figure 2 shows the energy conservation diagram and the phase-matching conditions. These relations can be written as

$$\omega_1 + \omega_2 - \omega_3 - \omega_4 = 0, \tag{1}$$

$$k_1 + k_2 + k_{\rm NL} - k_3 = 0, \tag{2}$$

$$k_4 - \Delta K = 0, \tag{3}$$

where $\omega_j\,(j = 1-4)$ is the angular frequency, $k_j\,(j = 1-4)$ is the propagation wave number, the subscripts 1–3 indicate the NIR optical waves, and the subscript 4 denotes the THz wave. $k_{\rm NL}$ is the phase mismatch induced by nonlinear self-phase modulation (SPM) and cross-phase modulation (XPM), and ΔK is the momentum uncertainty which can compensate the phase mismatch in the lateral direction of the optical fiber. There exist the relations between the four waves: $\omega_2 = \omega_1 - \omega_4$, $\omega_3 = 2\omega_2$. This configuration ensures that the frequency of the generated THz wave is equal to the difference frequency of the dual-wavelength laser, and then the THz frequency can be changed conveniently by tuning the difference frequency of the dual-wavelength laser.

A THz wave is generated when the energy conservation and phase-matching conditions are satisfied. Considering the material dispersion, waveguide dispersion and the nonlinear phase mismatch $k_{\rm NL}$, the calculated phase-matching curve and related pump wavelength λ_1 are shown in Fig. 3. When the pump wavelength λ_2 is near 1.55 μm, the related THz frequency is ~3.19 THz, and a 1.48–1.62 μm tuning range for λ_2 results in a 3.15–3.25 THz tuning range.

We assume that the z axis of the coordinate system is taken along the guide axis of the optical fiber, and all waves are polarized along the y axis. To stabilize the polarization states of the NIR optical waves, a polarization maintaining fiber should be used. It is shown that the polarization fluctuation of a fiber coil can be reduced by using a single-polarization single-mode optical fiber[14].

In the quasi-CW conditions, the four interaction waves can be written as

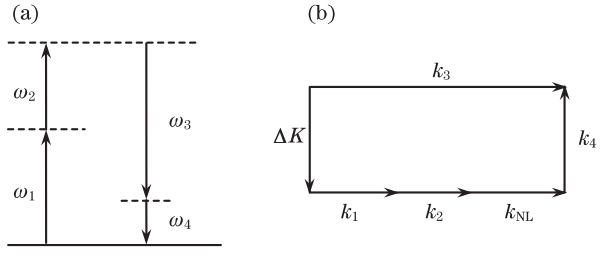

Fig. 2. Illustration of (a) energy-conservation diagram and (b) the phase-matching conditions for surface-emitted generation scheme.

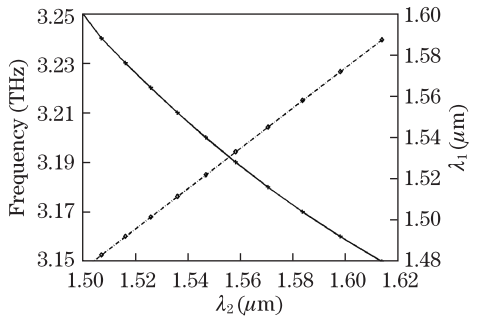

Fig. 3. Related THz frequency (solid line) and pump wavelength λ_1 (dashed line) depend on pump wavelength λ_2.

$$\mathbf{E}_j(\mathbf{r},t) = \frac{1}{2}\hat{y}F_j(x,y)A_j(z)\exp[\mathrm{i}(k_j z - \omega_j t)] + c.c., \quad (j = 1-3), \tag{4}$$

$$\mathbf{E}_4(\mathbf{r},t) = \frac{1}{2}\mathbf{A}_4(x,y,z)\exp(-\mathrm{i}\omega_4 t) + c.c., \tag{5}$$

where $A_j\,(j = 1-3)$ is the slowly varying envelope, $F_j\,(x,y)\,(j = 1-3)$ is the common transverse mode profile, $\hat{y}$ is the unit vector along the y axis. Using the basic propagation equation, it is straightforward to derive the coupled-wave equations for the three NIR optical waves propagating along the fiber[15]

$$\frac{\mathrm{d}A_1}{\mathrm{d}z} = \mathrm{i}\gamma_1(|A_1|^2 + 2|A_2|^2 + 2|A_3|^2)A_1, \tag{6}$$

$$\frac{\mathrm{d}A_2}{\mathrm{d}z} = \mathrm{i}\gamma_2(2|A_1|^2 + |A_2|^2 + 2|A_3|^2)A_2, \tag{7}$$

$$\frac{\mathrm{d}A_3}{\mathrm{d}z} = \mathrm{i}\gamma_3(2|A_1|^2 + 2|A_2|^2 + |A_3|^2)A_3, \tag{8}$$

where $\gamma_j\,(j = 1-3)$ is the nonlinear coefficient of the optical field with frequency ω_j. In writing these equations, the FWM-induced depletion of the NIR waves has been neglected, since the generated THz wave power is very weak compared with the power of the NIR waves.

From Eqs. (6)–(8), the solutions for the envelope of the NIR waves can be obtained as

$$A_1(z) = \sqrt{P_1}\exp[\mathrm{i}\gamma_1(P_1 + 2P_2 + 2P_3)z], \tag{9}$$

$$A_2(z) = \sqrt{P_2}\exp[\mathrm{i}\gamma_2(2P_1 + P_2 + 2P_3)z], \tag{10}$$

$$A_3(z) = \sqrt{P_3}\exp[\mathrm{i}\gamma_3(2P_1 + 2P_2 + P_3)z], \tag{11}$$

where $P_j = |A_j(0)|^2$, and P_1, P_2, P_3 are the incident NIR wave power at $z = 0$.

From Maxwell's equations, we obtain an inhomogeneous wave equation for the THz field as

$$(\nabla^2 + n_{\rm THz}^2 k_4^2)\mathbf{A}_4 = -\hat{y}\frac{3}{2}k_4^2\chi^{(3)}_{yyyy} F_1F_2F_3^*\sqrt{P_1P_2P_3}\exp(\mathrm{i}\beta z),$$

$$\beta = k_1 + k_2 + k_{\rm NL} - k_3,$$

$$k_{\rm NL} = \gamma_1(P_1 + 2P_2 + 2P_3) + \gamma_2(2P_1 + P_2 + 2P_3) + \gamma_3(2P_1 + 2P_2 + P_3), \tag{12}$$

where n_{THz} is the refractive index of the THz wave in fiber, β is the longitudinal phase mismatch factor. The phase mismatch in y direction is compensated by the momentum uncertainty, as mentioned before. To solve Eq. (12), we define a vector Green function $\mathbf{G}(x,y,z,\xi,\eta)$[16] by

$$(\nabla^2+n_{\mathrm{THz}}^2k_4^2)\mathbf{G}(x,y,z,\xi,\eta)=\hat{y}\delta(x-\xi)\delta(y-\eta)\exp(\mathrm{i}\beta z), \tag{13}$$

where δ is the Dirac delta function; then the solution of Eq. (12) is given by

$$\mathbf{A}_4(x,y,z)=-\frac{3}{2}k_4^2\chi_{yyyy}^{(3)}\sqrt{P_1P_2P_3}\iint F_1(\xi,\eta)F_2(\xi,\eta)F_3^*(\xi,\eta)\mathbf{G}(x,y,z,\xi,\eta)\mathrm{d}\xi\mathrm{d}\eta. \tag{14}$$

We first derive the Green function for $(\xi,\eta)=(0,0)$. Substituting $\mathbf{G}(x,y,z)=\mathbf{G}(x,y)\exp(\mathrm{i}\beta z)$ into Eq. (13), we obtain

$$(\nabla^2+\gamma^2)\mathbf{G}(x,y)=\hat{y}\delta(x)\delta(y)$$
$$\gamma=\sqrt{n_{\mathrm{THz}}^2k_4^2-\beta^2}=n_{\mathrm{THz}}k_4\cos\theta, \tag{15}$$

where $\theta\,(\approx 0)$ is the THz radiation angle with respect to the fiber's normal. The condition for the emission perpendicular to the fiber axis ($\theta=0$) is given by $\beta=0$, which means the phase matching is realized along the longitudinal direction. The Green function for Eq. (15) is[17]:

$$\mathbf{G}(x,y)=-\hat{y}\frac{\mathrm{i}}{4}H_0^2(\gamma r)\quad(r=\sqrt{x^2+y^2}), \tag{16}$$

where $H_0^{(2)}(\gamma r)$ is the Hankel function of the second kind. Then the Green function for $(\xi,\eta)=(0,0)$ can be written as

$$\mathbf{G}(x,y,z)=-\hat{y}\frac{\mathrm{i}}{4}H_0^{(2)}(\gamma r)\exp(\mathrm{i}\beta z)\cong\hat{y}\sqrt{\frac{1}{8\mathrm{i}\pi\gamma r}}\exp(-\mathrm{i}\gamma r)\exp(\mathrm{i}\beta z)\quad(\text{for }\ \gamma r>>1). \tag{17}$$

The Green function for $(\xi,\eta)\neq(0,0)$ can be obtained by shifting (x,y) coordinate. The radiated THz field can be calculated by integration of Eq. (14). The transverse mode profile $F_j(x,y)$ can be approximated by Gaussian function as

$$F_j(x,y)=\sqrt{\frac{4}{\pi n w^2}}(\frac{\mu_0}{\varepsilon_0})^{1/4}\exp[-(x^2+y^2)/w^2],\quad j=1-3, \tag{18}$$

where w is the $1/\mathrm{e}^2$ half widths of the modes, and n the linear refractive index. The same mode size was used for three NIR light waves. Substituting Eqs. (17) and (18) into Eq. (14), we obtain

$$\mathbf{A}_4(x,y,z)=\hat{y}\frac{-k_4^2\chi_{yyyy}^{(3)}\sqrt{2P_1P_2P_3}}{\pi w\sqrt{\mathrm{i}n^3n_{\mathrm{THz}}k_4r\cos\theta}}(\frac{\mu_0}{\varepsilon_0})^{3/4}\exp[\mathrm{i}(\beta z-\gamma r)]. \tag{19}$$

The power flow density of the THz radiation is given by $S_4=n_{\mathrm{THz}}\left|\mathbf{A}_4\right|^2/2\sqrt{\mu_0/\varepsilon_0}$ in the far field, we obtain from Eq. (19) the expression for the total radiated power out of the fiber core

$$P=\frac{k_4^3[\chi_{yyyy}^{(3)}]^2}{\pi w^2n^3}\frac{\mu_0}{\varepsilon_0}LP_1P_2P_3, \tag{20}$$

where L is the fiber length. Considering the collection ability of a cylindrical lens, the real detectable power will be one part of the quantity from the above expression.

We estimate the THz generation power by surface emitted FWM in the PM single-mode optical fiber. We assume the THz wave generation of 3.2 THz at radiation angle $\theta=0$. The fiber lasers can produce the 10-ns NIR pulses with the peak powers of 1 kW, the repetition rate is 100-kHz, corresponding to the average powers of 1 W. We also assume a conventional optical fiber made of fused silica with linear and nonlinear refractive indexes $n=1.45$ and $\tilde{n}_2=1\times10^{-22}$ m^2/V^2, respectively[18], and the mode radius of fiber is 4 μm. The other parameters are chosen as $n_{\mathrm{THz}}=2$, $L=100$ m. We obtain a generated THz-wave peak power ~4 mW, and the conversion efficiency is about 10^{-6}. This value is equivalent or greater than the conversion efficiency obtained by the second-order nonlinear optical methods such as DFG and OPO[19,20]. And there is some highly nonlinear fiber (HNLF) with the nonlinear refractive index $\tilde{n}_2$ of about 1×10^{-20} m^2/V^2, which are two orders larger than that of the usual single-mode fiber[21]. Then the generated THz power can be raised further by using the highly nonlinear optical fiber or increasing the pump power.

In conclusion, we propose a surface-emitted THz-wave source by FWM in a conventional single-mode optical fiber. Analytical expression of the output power is obtained. When the peak pump power is 1 kW, the related THz power is ~4 mW. It is a promising way to realize a miniaturized, easy-to-use, robust THz wave source.

This work was partially supported by the National "863" Program of China under Grant No. 2007AA804504.

References

1. D. Dragoman and M. Dragoman, Prog. Quant. Electron. **28,** 1 (2004).
2. Z. Chu, J. Liu, K. Wang, and J. Yao, Chin. Opt. Lett. **8,** 697 (2010).
3. P. Zhou and D. Fan, Chinese J. Lasers (in Chinese) **37,** 708 (2010).
4. J. Yao, N. Chi, P. Yang, H. Cui, J. Wang, J. Li, D. Xu, and X. Ding, Chinese J. Lasers (in Chinese) **36,** 2213 (2009).
5. Y. Ding, IEEE J. Quantum Electron. **13,** 705 (2007).
6. W. Shi, M. Leigh, J. Zong, and S. Jiang, Opt. Lett. **32,** 949 (2007).
7. T. Edwards, D. Walsh, M. Spurr, C. Rae, M. Dunn, and P. Browne, Opt. Express **14,** 1582 (2006).
8. J. Huillier, G. Torosyan, M. Theuer, Y. Avetisyan, and R. Beigang, App. Phys. B **86,** 185 (2007).
9. Y. Takushima, S. Shin, and Y. Chung, Opt. Express **15,** 14783 (2007).
10. Y. Sasaki, H. Yokoyama, and H. Ito, Electron. Lett. **41,** 712 (2005).

11. Y. Sasaki, A. Yuri, K. Kawase, and H. Ito, Appl. Phys. Lett. **81,** 3323 (2002).
12. Y. Sasaki, Y. Avetisyan, H. Yokoyama, and H. Ito, Opt. Lett. **30,** 2927 (2005).
13. C. Weiss, G. Torosyan, Y. Avetisyan, and R. Beigang, Opt. Lett. **26,** 563 (2001).
14. K. Takiguchi and K. Hotate, J. Lightwave. Technol. **11,** 1687 (1993).
15. G. P. Agrawal, *Nonlinear fiber optics,* 2nd ed. (Academic Press, San Diego, 1995).
16. T. Suhara, Y. Avetisyan, and H. Ito, IEEE J. Quant. Electron. **39,** 166 (2002).
17. A. Polyanin, "Helmholtz equation" http://eqworld. ipmnet. ru/en/solutions/lpde/lpde303.pdf (2004).
18. S. Takehito, W. Shi, and I. Yoh, Opt. Rev. **17,** 327 (2010).
19. T. Tanabe, S. Ragam, and Y. Oyama, Review of Scientific Instruments **80,** 113105 (2009).
20. R. Sowade, I. Breunig, I. Mayorga, J. Kiessling, C. Tulea, V. Dierolf, and K. Buse, Opt. Express **17,** 22303 (2009).
21. M. Asobe, T. Kanamori, and K. Kubodera, IEEE J. Quant. Electron. **29,** 2325 (1993).